Quaternary International
Volume 397, 18 March 2016, Pages 417–421
Japanese Quaternary Studies

Constraints on eustatic sea–level changes during the Mid-Pleistocene Climate Transition: evidence from the Japanese shallow-marine sediment record

Akihisa Kitamura
Institute of Geosciences, Shizuoka University, 836 Oya, Suruga-ku, Shizuoka, 422-8529, Japan

ABSTRACT

During the Middle Pleistocene, the nature of glacial–interglacial fluctuations changed from low-amplitude and a periodicity of 41 kyr to high-amplitude and quasi-periodic of 100 kyr. The origin of the Mid-Pleistocene Climate Transition (MPT) is an unsolved mystery. At present, there is a debate about whether the initiation of the MPT was a gradual or an abrupt process. This study investigated the process of initiation of the MPT from reconstructions of eustatic sea–level changes, as a proxy for global ice volume, based on a reexamination of lithofacies and fossil occurrences from shallow-marine sediments (the Omma Formation) exposed on the west coast of Japan. The Omma Formation comprises 19 depositional sequences spanning marine isotope stages (MIS) 56–21.3, reflecting sedimentation under alluvial plain to offshore conditions. The data indicate that (1) sea–level was lowest during MIS 22 (~0.9 Ma); (2) sea–level during MIS 34 (~1.13 Ma) and MIS 26 (~0.96 Ma) was lower than during any other glacial stage, except for MIS 22; and (3) sea–level during MIS 22 was at most 20 m lower than during MIS 34 and 26. Together, these findings suggest that the initiation of the MPT was a gradual, rather than abrupt, process.

1. Introduction

Glacial–interglacial cycles, and corresponding changes in eustatic sea-level, have had a considerable impact on both global climate and ecosystems throughout the Quaternary. Between 2.7 and 1.2 Ma, these cycles occurred with a periodicity of 41 kyr (the "41-kyr world"), and are attributed primarily to changes in the Earth's obliquity (Raymo and Nisancioglu, 2003; Huybers, 2006). In contrast, for the past 0.7 Myr, glacial cycles have followed an approximately 100-kyr periodicity (the "100-kyr world") (Hays et al., 1976; Imbrie et al., 1992). The timing of the glacial–interglacial cycles is explained by the theory postulated by Milankovitch in the early 20th century, which changes in boreal summer insolation are responsible for changes in the volume of boreal glacial ice sheets. However, the transition from the 41-kyr to the 100-kyr world, termed the Mid-Pleistocene Climate Transition (MPT) (e.g., Pisias and Moore, 1981), appears to bear no relation to orbital forcing. Furthermore, there is little agreement as to when the MPT occurred.

Clark et al. (2006) suggested that the constructed LR04 ''stacked'' benthic $\delta^{18}O$ record (Lisiecki and Raymo, 2005) (Fig. 1) shows the MPT beginning at ~1.25 Ma with a gradual increase in global ice volume and decrease in deep-water temperature. This hypothesis was supported by Sosdian and Rosenthal (2009), who reconstructed early Pleistocene eustatic sea–level (and hence global ice volume) changes with orbital-scale resolution using changes in the $\delta^{18}O$ of seawater based on analyses of $\delta^{18}O$ and Mg/Ca ratios of the epifaunal benthic foraminifera *Cibicidoides wuellerstorfi* and *Oridorsalis umbonatus* from North Atlantic Deep Sea Drilling Project (DSDP) site 607 (Fig. 1). However, Yu and Broecker (2010) questioned the result of Sosdian and Rosenthal (2009), because of the confounding influence of carbonate ion saturation on epifaunal benthic foraminiferal Mg/Ca ratios.

Recently, Elderfield et al. (2012) provided a record of eustatic sea–level for the past 1.5 Myr from Ocean Drilling Program (ODP) 181, site 1123, off New Zealand (Fig. 1). The record, based on $\delta^{18}O$ and Mg/Ca ratios of the shallow-infaunal benthic foraminifera *Uvigerina* spp. (the shells of which are barely affected by carbonate-ion saturation), suggests that the MPT was initiated by an abrupt increase in Antarctic ice volume at MIS 22 (~0.9 Ma). According to Elderfield et al. (2012), the uncertainty of the sea–level changes are ± 20 m. More recently, Rohling et al. (2014) reconstructed eustatic sea–level changes over the past 5.3 Myr using eastern Mediterranean planktonic foraminiferal $\delta^{18}O$ records. The authors reported a strong agreement between their reconstruction and the sea–level estimates of Elderfield et al. (2012), although the 95% probability interval of the Rohling et al. (2014) is ±6.3 m.

Prior to these studies, Bintanja et al. (2005) reconstructed the sea–level curve during the past 1.1 Myr from an ice-sheet–ocean-temperature model and the LR04 ‘‘stacked’’ benthic $\delta^{18}O$ record (Lisiecki and Raymo, 2005), although they did not discuss the pattern of initiation of the MPT. According to Bintanja et al. (2005), the uncertainty of their sea–level changes is ± 10 m.

Consequently, independent constraints on sea–level during the early Pleistocene glacial periods are required to help determine whether the initiation of the MPT was a gradual or an abrupt process. As the upper limits of U/Th dating and polar ice cores records are 0.5 Ma and 0.8 Ma, respectively, shelfal and nearshore sedimentary records provide useful constraints on eustatic sea–level changes during the early Pleistocene.

Existing shallow-water sediment records include those of the Wanganui Basin in New Zealand (Beu and Edwards, 1984; Abbott and Carter, 1994; Carter and Naish, 1998; Kondo et al., 1998), the Croton Basin in southern Italy (Rio et al., 1996; Massari et al., 1999, 2011), the Merced Formation in northern California (Carter et al., 2002), the Seoguipo Formation in southern Korea (Kim et al., 2010), and collisional marine foreland basin of southern Taiwan

(Chen et al., 2001) (Fig. 1). However, because these marine basins are too deep to detect small fluctuations in sea–level, none of these previous studies identified depositional sequences that correspond to MIS 22–24 in their lithostratigraphic schemes. In contrast, the depositional sequence in the Omma Formation, Central Japan, is firmly correlated with MIS 55–21 (Kitamura and Kawagoe, 2006) (Fig. 2) and thus encompasses this transitional period. To investigate the process of initiation of the MPT, this study reconstructed eustatic sea–level changes in glacial period, as a proxy for global ice volume, based on a reexamination of lithofacies and fossil occurrences from the Omma Formation.

2. Geological setting of depositional sequences in the Omma Formation

The Omma Formation is exposed around Kanazawa City, along the west coast of Central Japan (Fig. 1). The formation is up to 220 m thick in the type section along the Saikawa River at Okuwa. The Omma Formation overlies the middle Miocene Saikawa Formation (Ogasawara, 1977) and is in turn overlain unconformably by the Utatsuyama Formation (Ichihara et al., 1950) (Fig. 2). The marine Saikawa Formation is mainly composed of massive siltstone (Ogasawara, 1977). The Utatsuyama Formation is about 100 m thick and comprises fan-delta deposits of alternating beds of mudstone, coarse-grained sandstone, and conglomerate (Nirei, 1969).

Biostratigraphic and magnetostratigraphic data (Takayama et al., 1988; Ohmura et al., 1989; Sato and Takayama, 1992; Kitamura et al., 1994) indicate that the basement of the Omma Formation at the type section is located between the first occurrence (FO) of *Gephyrocapsa oceanica* (1.664 ± 0.025 Ma; Berger et al., 1994) and the FO of *Gephyrocapsa* (large) (1.515 ± 0.025 Ma; Berger et al., 1994) (Fig. 2). These data show that the top of the formation is located below the Brunhes–Matuyama magnetic polarity reversal (Fig. 2).

The Omma Formation has been divided into lower, middle, and upper parts (Fig. 2) (Kitamura et al., 1994, 2001). The lower and middle parts consist of 14 depositional sequences (Fig. 2, L1–L3, M1–11) that include the following architectural elements, in ascending stratigraphic order: (1) a basal sequence boundary that is superposed on the ravinement surface; (2) a transgressive systems tracts (TST) (2–5 m thick) consisting of a basal shell bed of 0.3 m thick (a condensed onlap shell bed) overlain by fine- to very-fine-grained sandstone; (3) a maximum flooding horizon coinciding with the horizon with the highest concentration of sand-size carbonate grains; (4) a highstand systems tracts (HST) (2–3 m thick) consisting of fine-grained sandstone and sandy siltstone; and (5) a regressive systems tracts (RST) (<1 m thick) comprising fine-grained sandstone with a coarsening-upward trend (Kitamura et al., 2000). The upper part of the formation consists of five depositional sequences (Fig. 2, U1–U5) associated with back-marsh to inner-shelf environments (Kitamura and Kawagoe, 2006). Erect stumps and tracks of elephants and deers have been found from back-marsh deposits (Kitamura and Kawagoe, 2006). These parts of the Omma Formation show no progressive shift in litho- and biofacies toward deeper or shallower deposits.

Except for four depositional sequences in the upper part, during the deposition of each sequence, the molluscan fauna changed from cold-water, upper-sublittoral species to warm-water, lower-sublittoral species, followed by a return to cold-water, upper-sublittoral species (Kitamura et al., 1994). The term “cold-water species” is applied to fauna living in the area north of southern Hokkaido and/or in water deeper than 150–160 m off Sanin and Hokuriku. These species are present in the Pacific coast area north of the Boso Peninsula at 35°N, where the warm Kuroshio Current diverges away from the Japanese Islands. The term “warm-water species” is applied to fauna living in the area south of southern Hokkaido, and living at the area shallower than 150–160 m depth off Sanin and Hokuriku. The area off Sanin

and Hokuriku is strongly influenced by the warm Tsushima Current, which is a branch of the warm Kuroshio Current. These species are present south of 35°N on the Pacific coast of Japan. The cyclic changes in molluscan content in these depositional sequences indicate that ocean conditions and water depth fluctuated concurrently. Specifically, increased water depths correspond to periods of warmer marine conditions associated with the inflow of the warm Tsushima Current. Thus, the depositional sequences of the Omma Formation are correlated with obliquity-driven glacio-eustatic changes, with a periodicity of 41 kyr (Kitamura et al., 1994). Kitamura and Kimoto (2006) correlated 19 depositional sequences in the Omma Formation with oxygen isotope stages 56 to 21.3 using a combination of sequence stratigraphic, biostratigraphic, and magneto stratigraphic data (Fig. 2). As noted above, the Omma Formation contains only shallow-marine facies that can be perfectly correlated between oxygen isotope stages and depositional sequences during MIS 55–21.

3. Sea–level reconstruction

Water depth in sedimentary basins can be influenced by several factors, including compaction, basement subsidence, sediment supply, hydro-isostatic effects, and eustatic sea–level changes. The basement rock on which the Omma Formation was deposited (i.e., the Saikawa Formation sediments) was consolidated prior to deposition of the Omma Formation, since the lower unconformity is penetrated by marine rock-boring bivalves (Kitamura, 1997). The sediments of the Omma Formation are unconsolidated and consist primarily of very-fine- to fine-grained sandstone, with a burial depth equal to the total formation thickness (210 m). From the porosity–depth relationship (Sclater and Christie, 1980; Ramm and Bjiørlykke, 1994), sandstone porosity within the formation decreases by only 5% from the surface to a burial depth of 250 m, indicating that the water–depth curve is only weakly affected by compaction.

With the exception of depositional sequence U4 (DS U4), which corresponds to MIS 22–21.4 (Kitamura and Kawagoe, 2006), the sequence boundaries for the depositional sequences of the Omma Formation coincide with ravinement surfaces formed by shoreface erosion during marine transgression (Bruun, 1962). As the depth of shoreface erosion is generally less than 40 m (e.g., Saito, 1989), water depths at sequence boundaries probably remained at least than 40 m for the 800-kyr period between MIS 56 and 21.3, indicating that basin subsidence kept pace with sediment supply.

Being located far from the former continental ice-sheets, the marine basin of the Omma Formation was influenced by hydro-isostasy alone, in which rising (falling) sea–level causes basin subsidence (uplift) due to increasing (decreasing) water load. Consequently, relative sea–level during glacial periods can be compared directly, allowing water-depth changes represented by the Omma Formation to be used as a proxy for eustatic sea–level changes.

Water depth change, as recorded by the Omma Formation, has been reconstructed by analyses of lithofacies and fossil occurrences (Kitamura, 1991; Kitamura et al., 1994; Kitamura and Kawagoe, 2006; Kitamura and Kimoto, 2006) (Fig. 2). Non-marine sediments, comprising back-marsh deposits found in the lowest levels of DS U4 (MIS 22), suggest that sea–level during MIS 22 was lower than at any other time between MIS 56 and 21 (Kitamura and Kawagoe, 2006). Kitamura and Kimoto (2004) and Kitamura and Kawagoe (2006) described well-sorted, fine-sand units that contain parallel laminations or hummocky cross-stratification in the upper levels of depositional sequences 8 and U1, corresponding to MIS 36–34 and 28–26, respectively (Fig. 2). These sediments do not contain fossils such as molluscs and foraminifera, due to the dissolution of calcareous shell materials. Sedimentary structures indicate that the sediments were deposited in a lower shoreface environment. Because the fair-weather wave base lies at depths of about 5–15 m (Walker and Plint, 1992), the depth of the lower shoreface is

169 inferred to be 5–15 m. The reexamination herein indicates that, with the exception of MIS 22,
170 sea–level was lower during MIS 34 (~1.13 Ma) and 26 (~0.96 Ma) than during any other glacial
171 stage between MIS 56 and 21.
172
173 **4. Discussion and conclusion**
174 Based on a reexamination of lithofacies and fossil occurrences from the shallow-marine
175 Omma Formation, sea–level was lower during MIS 22 than at any other time between MIS 56
176 and 21. This finding is in close agreement with the findings of Bintanja et al. (2005), Elderfield
177 et al. (2012), and Rohling et al. (2014), and supports the argument for a significant increase in
178 global ice volume at MIS 22, referred to by Clark et al. (2006) as the 900-ka event.
179 This reexamination also indicates that sea–level was lower during MIS 34 and 26 than
180 during other glacial stages (except for MIS 22) of the same time period, in agreement with the
181 conclusion of Bintanja et al. (2005). According to Elderfield et al. (2012) and Rohling et al.
182 (2014), sea–level in MIS 34 and 26 was not significantly lower than in the other glacial periods
183 between MIS 56 and 21. This is inconsistent with the new evidence of the present study.
184 The differences in sea–level between MIS 22 and the two glacial stages MIS 34 and 26 are
185 estimated to have been 20 m (Bintanja et al., 2005), 40 m (Rohling et al., 2014) or 50 m
186 (Elderfield et al., 2012) (Fig. 2). As noted above, the water depth is thought to have been
187 between 5 and 15 m during MIS 34 and 26. Conversely, the sea–level during MIS 22 is
188 uncertain, because the study area emerged and was a back-marsh environment during this period
189 (Fig. 2). When the difference in sea–level of 50 m (20 m) is applied, the elevation of the study
190 area is estimated to have been 35–45 m (5–15 m) during MIS 22. As back-marsh commonly
191 develops in low coastal plains, it is likely that the difference in sea–level was 20 m, as
192 determined by Bintanja et al. (2005), rather than the 40–50 m estimated by Elderfield et al.

193 (2012) and Rohling et al. (2014).

194 As noted above, the uncertainties in estimates of sea–level from geochemical data range
195 from ±6.3 m to ±20 m (Bintanja et al., 2005; Elderfield et al., 2012; Rohling et al., 2014). In
196 contrast, as hydrographic conditions change drastically from shoreface to offshore, lithofacies
197 are highly sensitive to changes in sea–level during sea–level low stands. It is therefore likely
198 that the inconsistency between this study and the geochemical studies of Elderfield et al. (2012)
199 and Rohling et al. (2014) reflect uncertainties in the estimates from geochemical data.

200 This means that the early Pleistocene sea–level curve of Bintanja et al. (2005) is more
201 suitable than those of Elderfield et al. (2012) and Rohling et al. (2014), and that the initiation of
202 the MPT was a gradual (e.g., Clark et al., 2006), rather than abrupt, process (Elderfield et al.,
203 2012).

204

205 **Acknowledgments**

206 I thank three anonymous reviewers, whose comments and suggestions improved the original
207 manuscript.

208

209 **References**

210 Abbott, S.T., Carter, R.M., 1994. The sequence architecture of mid-Pleistocene (0.35–0.95 Ma)
211 cyclothems from New Zealand: facies development during a period of orbital control on
212 sea–level cyclicity. In: de Boer, P.L., Smith, D.G. (Eds.), Orbital Forcing and Cyclic
213 Sequences. International Association of Sedimentologist Special Publication 19, 367–394.

214 Berger, W.H., Yasuda, M.K., Bickert, T., Wefer, G., Takayama, T., 1994. Quaternary time scale

215 for the Ontong Java Plateau: Milankovitch template for Ocean Drilling Program Site 806.
216 Geology 22, 463–467.
217 Beu, A.G., Edwards, A.R., 1984. New Zealand Pleistocene and late Pliocene glacio-eustatic
218 cycles. Palaeogeography, Palaeoclimatology, Palaeoecology 46, 119–142.
219 Bintanja, R., van de Wal R.S.W., Oerlemans, J., 2005. Modelled atmospheric temperatures and
220 global sea levels over the past million years. Nature 437, 125–128.
221 Bruun, P., 1962. Sea level rise as a cause of shoreface erosion. Journal of the Waterways and
222 Harbors Division: proceedings of the American Society of Civil Engineers 88, 117–130.
223 Carter, R.M., Naish, T.R., 1998. A review of Wanganui Basin, New Zealand: global reference
224 section for shallow marine, Plio-Pleistocene (2.5-0 Ma) cyclostratigraphy. Sedimentary
225 Geology 122, 37–52.
226 Carter, R.M., Abbott, S.T., Graham, I.J., Naish, T.R., Gammon, P.R., 2002. The middle
227 Pleistocene Merced-2 and -3 sequences from Ocean Beach, San Francisco, Sedimentary
228 Geology 153, 23–41.
229 Chen, W.S., Ridgway, K.D., Horng, C.S., Chen, Y.G., Shea, K.S., Yeh, M.G., 2001. Stratigraphic
230 architecture, magnetostratigraphy, and incised-valley systems of the Pliocene-Pleistocene
231 collisional marine foreland basin of Taiwan. Geological Society of America Bulletin 113,
232 1249-1271.

233 Clark, P.U., Archer, D., Pollard, D., Blum, J.D., Rial, J.A., Brovkin, V, Mix, A.C., Pisias, N.G.
234 and Roy, M., 2006 The middle Pleistocene transition: characteristics, mechanisms, and
235 implications for long-term changes in atmospheric pCO_2. Quaternary Science Reviews 25,
236 3150–3184.
237 Elderfield, H., Ferretti, P., Greaves, M., Crowhurst, S., McCave, I.N., Hodell, D., Piotrowski,
238 A.M., 2012. Evolution of ocean temperature and ice volume through the mid-Pleistocene
239 climate transition. Science 337, 704–709.
240 Hays, J.D., Imbrie, J., Shackleton, N.J., 1976. Variations in the Earth's orbit: pacemarker of the
241 ice ages. Science 194, 1121–1132.
242 Huybers, P., 2006. Early Pleistocene glacial cycles and the integrated summer insolation
243 forcing. Science 313, 508–511.
244 Ichihara, M., Ishio, G., Morishita, A., Nakagawa, T., Tsuda, K., 1950. Geological study of
245 the Toyama and Ishikawa Prefectures. No. 2, Kanazawa, Isurugi and Fukumitsu provinces.
246 Chigaku 2, 17–27 [in Japanese].
247 Imbrie, J., Boyle, E.A., Clemens, S.C., Duffy, A., Howard, W.R., Kukla, G., Kutzbach, J.,
248 Martinson, D.G., McIntyre, A., Mix, A.C., Molfino, B., Morley, J.J., Peterson, L.C., Pisias,
249 N.G., Prell, W.L., Raymo, M.E., Shackleton, N.J., Toggweiler, J.R., 1992. On the structure
250 and origin of major glaciation cycles. 1. Linear responses to Milankovitch forcing.

Paleoceanography 7, 701–738.

Kim, J.K., Khim, B.-K., Woo, K.S., Yoon, S.H. 2010: Records of palaeo-seawater condition from oxygen-isotope profiles of early Pleistocene fossil molluscs from the Seoguipo Formation (Korea). Lethaia 43, 170–181.

Kitamura, A., 1991. Paleoenvironmental transition at 1.2 Ma in the Omma Formation, Central Japan. Transactions and Proceedings of the Palaeontological Society of Japan. 162, 767–780.

Kitamura, A., 1997. The lower unconformity and molluscan fossils of the basal part of the early Pleistocene Omma Formation at its type section, Ishikawa Prefecture, central Japan. The Journal of the Geological Society of Japan 103, 763–769 [Japanese with English abstract].

Kitamura, A., 1998, Glaucony and carbonate grains as indicators of the condensed section: Omma Formation, Japan. Sedimentary Geology 122, 151–163.

Kitamura, A., Kondo, Y., Sakai, H., Horii, M., 1994, Cyclic changes in lithofacies and content in the early Pleistocene Omma Formation, Central Japan related to the 41,000-year orbital obliquity. Palaeogeography, Palaeoclimatology, Palaeoecology 112, 345–361.

Kitamura, A., Matsui, H., Oda, M., 2000. Constraints on the timing of systems tract development with respect to sixth-order (41 ka) sea–level changes: an example from the Pleistocene Omma Formation, Sea of Japan. Sedimentary Geology 131, 67–76.

Kitamura, A., Takano, O., Takada, H., Omote, H., 2001, Late Pliocene-early Pleistocene paleoceanographic evolution of the Sea of Japan. Palaeogeography, Palaeoclimatology, Palaeoecology 172, 81–98.

Kitamura, A., Kawagoe, T., 2006, Eustatic sea–level change at the mid-Pleistocene climate

transition: New evidence from the Japan shallow-marine sediment record. Quaternary Science Review 25, 323–335.

Kitamura, A., Kimoto, K., 2006. History of the inflow of the warm Tsushima Current into the Sea of Japan between 3.5 and 0.8 Ma. Palaeogeography, Palaeoclimatology, Palaeoecology 236, 355–366.

Kondo, Y., Abbott, S.T., Kitamura, A., Naish, T., Kamp, P.J.J., Kamataki, T., Saul, G.S., 1998. The relationship between shellbed type and sequence architecture: Examples from Japan and New Zealand. Sedimentary Geology 122, 109–127.

Lisiecki, E.L., Raymo, E.R., 2005, A Pliocene-Pleistocene stack of 57 globally distributed benthic $\delta^{18}O$ records. Paleoceanography 20, PA1003, doi:10.1029/2004PA001071.

Massari, F., Sgavetti, M., Rio, D., D' Alessandro, A., Prosser. G., 1999. Composite sedimentary record of falling stages of Pleistocene glacio-eustatic cycles in a shelf setting (Crotone basin, south Italy). Sedimentary Geology 127, 85–110.

Massari, F., Rio, D., Sgavetti, M., Prosser, G., D'Alessandro, A., Asioli, A., Capraro, L., Fornaciari, E., Tateo, F., 2011. Interplay between tectonics and glacio-eustasy: Pleistocene succession of the Crotone basin, Calabria (southern Italy). Geological Society of America Bulletin 114, 1183–1209.

Nirei, H., 1969. On the Utatsuyama Formation around Kanazawa City, Central Japan. The Journal of the Geological Society of Japan 75, 471–484 [in Japanese with English abstract].

Ogasawara, K., 1977. Paleontological analysis of Omma Fauna from Toyama-Ishikawa area,

293 Hokuriku Province, Japan. Science Reports of the Tohoku University, Second Series,
294 Geology 47, 43–156.
295 Ohmura, I., Ito, T., Masaeda, H., Danbara, T., 1989. Magnetostratigraphy of the Omma
296 Formation distributed in Kanazawa City, Ishikawa Prefecture, central Japan. Professor H.
297 Matsuo Memoir 111-124 [Japanese with English abstract].
298 Pisias, N.G., Moore, Jr., T.C., 1981. The evolution of Pleistocene climate: a time series
299 approach. Earth and Planetary Science Letters 52 450–458.
300 Ramm, M., Bjiørlykke, K., 1994. Porosity/depth trends in reservoir sandstones: Assessing the
301 quantitative effects of varying pore-pressure, temperature history and mineralogy,
302 Norwegian Shelf Data. Clay Minerals 24, 475–490.
303 Raymo, M.E., Nisancioglu, K., 2003. The 41 kyr world: Milankovitch's other unsolved mystery.
304 Paleoceanography 18, doi:10.1029/2002PA000791.
305 Rio, D., Channell, J.E.T., Massari, F., Poli, M.S., Sgavetti, M., D'Alessandro, A., Prosser, G.,
306 1996. Reading Pleistocene eustasy in a tectonically active siliciclastic shelf setting (Crotone
307 peninsula, southern Italy). Geology 24, 743–746.
308 Rohling, E.J., Foster, G.L., Grant, K.M., Marino, G., Roberts, A.P., Tamisiea, M.E., Williams, F.,
309 2014. Sea–level and deep-sea-temperature variability over the past 5.3 million years. Nature
310 508, 477–482.

311 Saito, Y., 1989. Modern storm deposits in the inner shelf and their recurrence intervals, Sendai
312 Bay, northeast Japan. In: Taira, A., Masuda, F. (Eds.), Sedimentary facies in the active plate
313 margin. Terra Scientific Publishing Company, Tokyo, 331–344.
314 Sato, T., Takayama, T., 1992. A stratigraphically significant new species of the calcareous
315 nannofossil Reticulofenestra asanoi. In: Ishizaki, K., Saito, T., (Eds.), Centenary of Japanese
316 Micropaleontology, Terra Scientific Publishing Company, Tokyo, 457–460.
317 Sclater, J.G., Christie, P.A.F., 1980. Continental stretching: an explanation of the post
318 Mid-Cretaceous subsidence of the central North Sea basin. Journal Geophysical Research 85,
319 3711–3739.
320 Sosdian, S., Rosenthal, Y., 2009. Deep-sea temperature and ice volume changes across the
321 Pliocene-Pleistocene climate transitions. Science 325, 306–310.
322 Takayama, T., Kato, M., Kudo, T., Sato, T., Kameo, K., 1988. Calcareous microfossil
323 biostratigraphy of the uppermost Cenozoic formations distributed in the coast of the
324 Japan Sea, Part 2: Hokuriku sedimentary basin. Journal of the Japanese Association for
325 Petroleum Technology 53, 9–27 [Japanese with English abstract].
326 Walker, R.G., Plint, A.G., 1992. Wave- and storm-dominated shallow marine systems. In Walker,
327 R.G., James, N.P. (Eds). Facies models: Response to sea level change. Geological
328 Association of Canada 219–238.

329 Yu, J., Broecker, W. S., 2010. Comment on “Deep-sea temperature and ice volume changes

330 across the Pliocene-Pleistocene climate transitions” Science 328, 1480c.

331

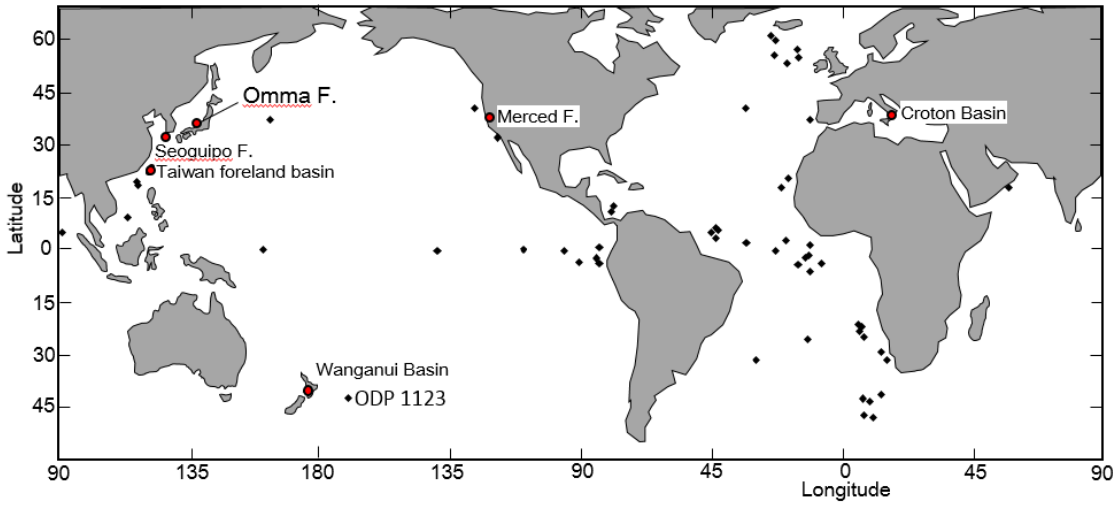

Figure 1 Locations of deep-sea cores (diamond symbols) used in the LR04 ‘‘stacked’’ benthic $\delta^{18}O$ record (Lisiecki and Raymo, 2005), location of ODP 1123 (Elderfield et al., 2012), and locations of early Pleistocene shelfal and nearshore sedimentary records (circles).

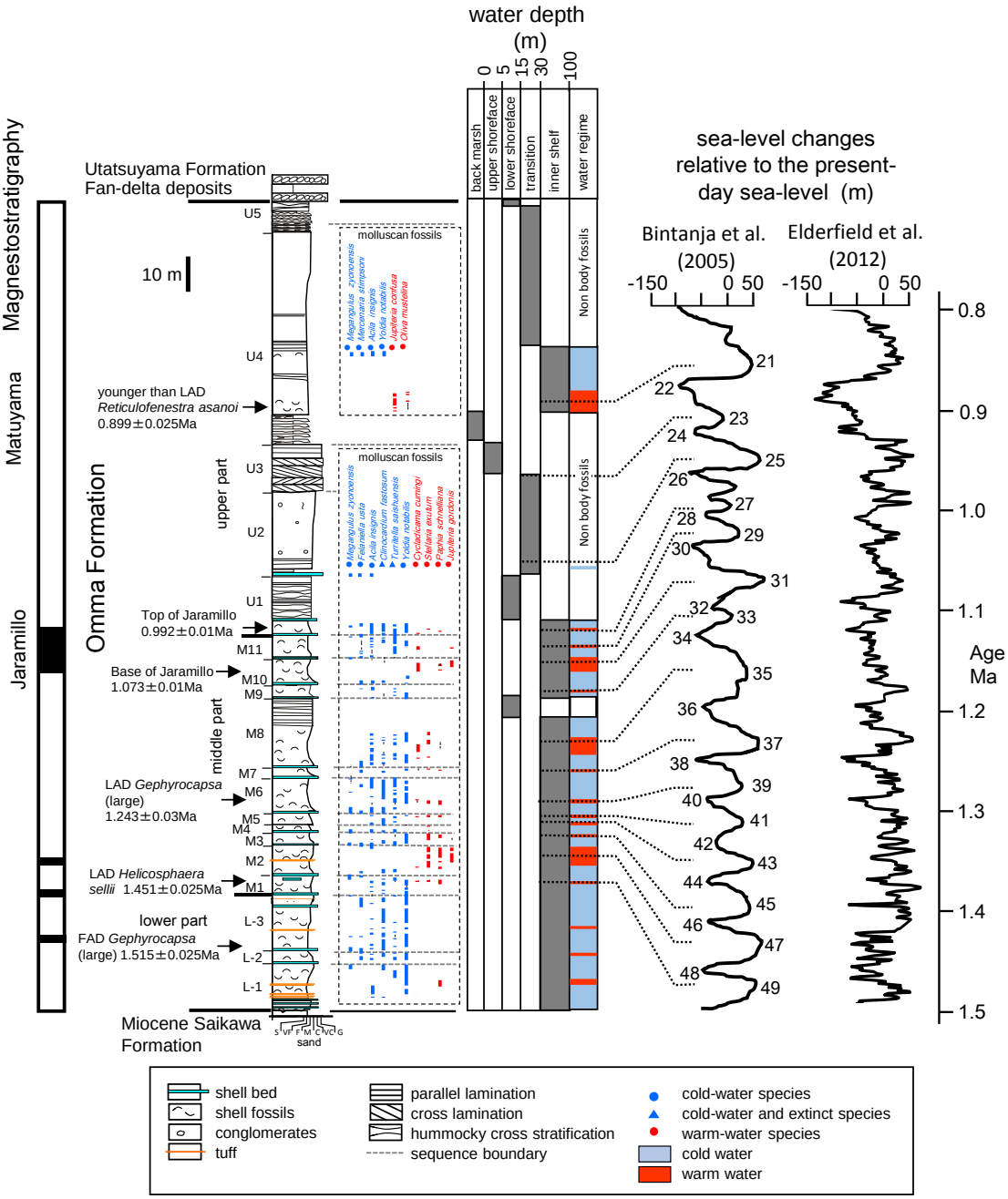

Figure 2 Columnar section of the Omma Formation at its type section along the Saikawa River at Okuwa. Comparison of water-depth changes reconstructed from the Omma Formation and eustaic sea–level changes inferred from geochemical signals of benthic foraminifera in deep-sea sediments (Bintanja et al., 2005; Elderfield et al., 2012).